Title

Quantitative two-dimensional ultrashort echo time magnetization transfer (2D UTE-MT) imaging of cortical bone

Journal

Magnetic Resonance in Medicine, 79(4)

ISSN

0740-3194

Authors

Ma, Ya-Jun
Tadros, Anthony
Du, Jiang
et al.

Publication Date

2018-04-01

DOI

10.1002/mrm.26846

FULL PAPER

Magnetic Resonance in Medicine 00:00–00 (2017)

Quantitative Two-Dimensional Ultrashort Echo Time Magnetization Transfer (2D UTE-MT) Imaging of Cortical Bone

Ya-Jun Ma,[1†] Anthony Tadros,[1†] Jiang Du,[1] and Eric Y. Chang[1,2]*

Purpose: To investigate quantitative 2D ultrashort echo time magnetization transfer (UTE-MT) imaging in ex vivo bovine cortical bone and in vivo human tibial cortical bone.

Methods: Data were acquired from five fresh bovine cortical bone samples and five healthy volunteer tibial cortical bones using a 2D UTE-MT sequence on a clinical 3T scanner. The 2D UTE-MT sequence used four or five MT powers with five frequency offsets. Results were analyzed with a two-pool quantitative MT model, providing measurements of macromolecular fraction (f), macromolecular proton transverse relaxation times (T_{2m}), proton exchange rates from water/macromolecular to the macromolecular/water pool (RM_{0m}/RM_{0w}), and spin-lattice relaxation rate of water pool (R_{1w}). A sequential air-drying study for a small bovine cortical bone chip was used to investigate whether above MT modeling parameters were sensitive to the water loss.

Results: Mean fresh bovine cortical bone values for f, T_{2m}, R_{1w}, RM_{0m}, and RM_{0w} were $59.9 \pm 7.3\%$, $14.6 \pm 0.3\,\mu s$, $9.9 \pm 2.4\ s^{-1}$, $17.9 \pm 3.6\ s^{-1}$, and $11.8 \pm 2.0\ s^{-1}$, respectively. Mean in vivo human cortical bone values for f, T_{2m}, R_{1w}, RM_{0m} and RM_{0w} were $54.5 \pm 4.9\%$, $15.4 \pm 0.6\,\mu s$, $8.9 \pm 1.1\ s^{-1}$, $11.5 \pm 3.5\ s^{-1}$, and $9.5 \pm 1.9\ s^{-1}$, respectively. The sequential air-drying study shows that f, RM_{0m}, and R_{1w} were increased with longer drying time.

Conclusion: UTE-MT two-pool modeling provides novel and useful quantitative information for cortical bone. **Magn Reson Med 000:000–000, 2017. © 2017 International Society for Magnetic Resonance in Medicine.**

Key words: ultrashort echo time; magnetization transfer; two-pool modeling; cortical bone

INTRODUCTION

Osteoporotic fractures, such as of the hip and vertebra, have a very high morbidity and mortality (1). With a lifetime risk of approximately 40% to 50% for women and 13% to 22% for men, osteoporotic fractures are generally defined as occurring at sites of low bone mineral density (BMD) (2). Although BMD is considered the standard measure for the diagnosis of osteoporosis and assessment of fracture risk, several studies have demonstrated that BMD cannot be used as the sole predictor of bone strength. In particular, changes in BMD have been shown to account for <50% of variation in whole bone strength (3), with the majority of fragility fractures occurring in patients with a T-score > -2.5 (4,5). Identification of more sensitive determinants of bone strength using MRI has consequently been an active area of interest.

Because of the short T_2 components of bone matrix, clinical MRI systems are generally limited to the imaging of the marrow space. While high resolution MRI has been shown to detect age and disease-induced changes in trabecular morphology (6), the use of ultrashort echo time (UTE) pulse sequences has allowed for the quantitative evaluation of cortical bone (7–10). Water content and T_2^* measurements have been shown to correlate with cortical bone porosity and failure properties (8,10). Despite that, protons with extremely fast transverse relaxation, such as tightly bound water and collagen protons, remain undetectable even when UTE is used. Magnetization transfer (MT) imaging has therefore been investigated as a potential method to indirectly assess these "invisible" proton pools.

The MT technique generates unique contrast and quantitative information in MRI by exploiting coupling processes between macromolecular and mobile protons. MT imaging uses an off-resonance radiofrequency (RF) pulse to preferentially saturate macromolecular protons. Because macromolecular protons can influence the spin state of mobile protons, this off-resonance saturation can be subsequently transferred to mobile protons and thereby be measured by MRI. The extent of magnetization transfer between these two pools of protons depends on their rate of exchange (11). In combination with UTE (UTE-MT), MT has been studied as a quantitative measure of short T_2 tissues (12,13). More recently, magnetization transfer ratios (MTR) using the UTE-MT technique have been shown to be sensitive to cortical bone porosity, as determined by micro-CT and biomechanical function (14).

To improve the sensitivity and reproducibility of MT metrics in cortical bone, we sought to explore a more quantitative modeling of MT phenomena in combination with UTE. We aimed to optimize acquisition protocols and better understand MT behavior in ex vivo bovine and in vivo healthy human tibial cortical bone. Our purpose was to establish methods enabling UTE-MT two-pool modeling measurements that might potentiate new surrogate markers for cortical bone strength.

[1]Department of Radiology, University of California, San Diego, San Diego, California, USA.

[2]Radiology Service, VA San Diego Healthcare System, San Diego, California, USA.

Grant sponsor: GE Healthcare; Grant sponsor: NIH; Grant numbers: 1R01 AR062581 and 1R01 AR068987; Grant sponsor: VA Clinical Science R&D Service; Grant number: 1I01CX001388.

*Correspondence to: Eric Y. Chang, MD, VA San Diego Healthcare System, San Diego, CA 92161, USA. E-mail: ericchangmd@gmail.com.

†These authors contributed equally to this work.

Received 6 January 2017; revised 28 June 2017; accepted 30 June 2017

DOI 10.1002/mrm.26846

Published online 00 Month 2017 in Wiley Online Library (wileyonlinelibrary.com).

METHODS

Two-Pool MT Modeling

Two-pool MT modeling was carried out to measure macromolecular fraction (f), water proton transverse relaxation time (T_{2w}), macromolecular proton transverse relaxation time (T_{2m}), proton exchange from water to macromolecular pool (RM_{0m}), and proton exchange from the macromolecular to water pools (RM_{0w}). Two-pool UTE-MT modeling was largely based on the previously described Ramani model (15), in which the MT pulse was treated as a rectangular continuous wave (CW) signal with the same mean saturating power as the experimentally used shaped pulse, or the so-called continuous wave power equivalent (CWPE) approximation. The angular frequency of precession w_{CWPE} induced by the off-resonance MT pulse was used to measure the amplitude of the B_1 field. The UTE-MT signal was modeled by the following equation (15):

$$S = gM_{0w}\frac{R_{1m}\left[\frac{RM_{0w}f}{R_{1w}(1-f)}\right] + R_{RFm} + R_{1m} + RM_{0w}}{\left[\frac{RM_{0w}f}{R_{1w}(1-f)}\right](R_{1m}+R_{RFm}) + \left(1+\left[\frac{w_{CWPE}}{2\pi\Delta f}\right]^2\left[\frac{1}{R_{1w}T_{2w}}\right]\right)(R_{RFm}+R_{1m}+RM_{0w})}, \quad [1]$$

in which M_{0m} and M_{0w} are the fully relaxed magnetizations of macromolecular and water pools, respectively. f is defined as $\frac{M_{0m}}{M_{0m}+M_{0w}}$. R_{1m} and R_{1w} are the corresponding longitudinal rate constants. g is an amplitude scaling factor. R is the first-order magnetization exchange rate constant between the two pools. R_{RFm} is the loss rate of longitudinal magnetization of the macromolecular pool caused by the RF saturation of the MT pulse. Here, we use a Gaussian line shape for the macromolecular proton pool in cortical bone because of its extremely short T_2 value (16). Additional details regarding the UTE-MT two-pool modeling used in this study have been previously reported (17).

Pulse Sequence

The 2D UTE-MT sequence uses an MT preparation pulse followed by a basic 2D UTE data acquisition. The basic 2D UTE sequence uses a hard pulse or a short half pulse excitation followed by 2D radial ramp sampling. Fast transmit/receive switching allows for a minimal nominal echo time of approximately 10 μs (14). The MT preparation pulse is a Fermi pulse with a duration of 8 ms, a spectral bandwidth of 0.8 kHz, a maximal B_1 of 24 μT, and a maximal saturation flip angle of 1740°. The Fermi pulse was used because it provided an improved spectral profile compared with a rectangular pulse and higher efficiency compared with conventional Gaussian or sinc pulses, facilitating MT modeling of cortical bone, which has an extremely short apparent transverse relaxation time or T_2^*. 2D UTE-MT data were acquired with a series of MT pulse frequency offsets (Δf) and powers (ω_1) for two-pool MT modeling.

Ex Vivo UTE-MT Imaging

In total, five mature bovine femoral and tibial midshafts from freshly slaughtered animals were obtained from a local slaughterhouse and cleaned of external muscle and soft tissue. A bovine cross-section with approximate thickness of 4 cm was cut from each specimen using a low-speed diamond saw (Isomet 1000, Buehler, Lake Bluff, IL, USA) with constant water irrigation and stored in phosphate buffered saline (PBS) solution for 24 h before use. A wrist coil (BC-10, Medspira, Minneapolis, MN) was used for both signal excitation and reception. The 2D non-selective UTE-MT imaging protocol included: pulse repetition time (TR) = 100 ms, echo time = 10 μs, field of view = $8 \times 8\,cm^2$, hard excitation pulse (32 μs) with a flip angle = 10°, acquisition matrix = 128×128, five MT powers (300°, 600°, 900°, 1200°, and 1500°), and five MT frequency offsets (2, 5, 10, 20, and 50 kHz), with a total of 25 different MT data sets. The total scan time was approximately 17.5 min. T_1 values were measured with the same UTE sequence except without MT preparation using a rectangular excitation pulse (duration = 80 μs) with a flip angle = 25° and multiple TRs (i.e., 24, 50, 100, 200, 400, 600, 800 ms). T_1 was calculated by fitting the following equation (18,19):

$$S = S_0 e^{-\frac{TE}{T_2}}\frac{1-e^{-\frac{TR}{T_1}}}{1-\cos(\theta)e^{-\frac{TR}{T_1}}}. \quad [2]$$

where S_0 is the signal intensity in the equilibrium state and echo time (TE) is a constant. Therefore, the first two elements in the above equation can be combined into a constant when fitting. Total scan time was approximately 15.2 min.

A sequential air-drying study was also carried out to investigate whether UTE-MT modeling parameters are sensitive to the water content loss in cortical bone. A bovine cortical bone chip was cut with approximate dimensions of $18 \times 12 \times 5\,mm^3$. The bone chip was immersed in PBS for 30 mins before the first experiment. The second and third experiments were conducted after 1 and 3 h of air drying in a 22°C condition, respectively. A 30-mL birdcage coil was used for both RF transmission and signal reception. The sequence parameters were identical to the above bovine cortical bone sample study.

Reproducibility was investigated for the two-pool UTE-MT modeling of cortical bone with three measurements. The MRI system was reset before each measurement and the same slice location was used for all the measurements. Mean and standard deviation values of the three independent measurements were calculated.

In Vivo UTE-MT Imaging

The 2D UTE-MT sequence was also applied to the tibial midshaft of five healthy volunteers (all males, 28 to 43 years old, mean/standard deviation = 32.6 ± 6.4 y) for

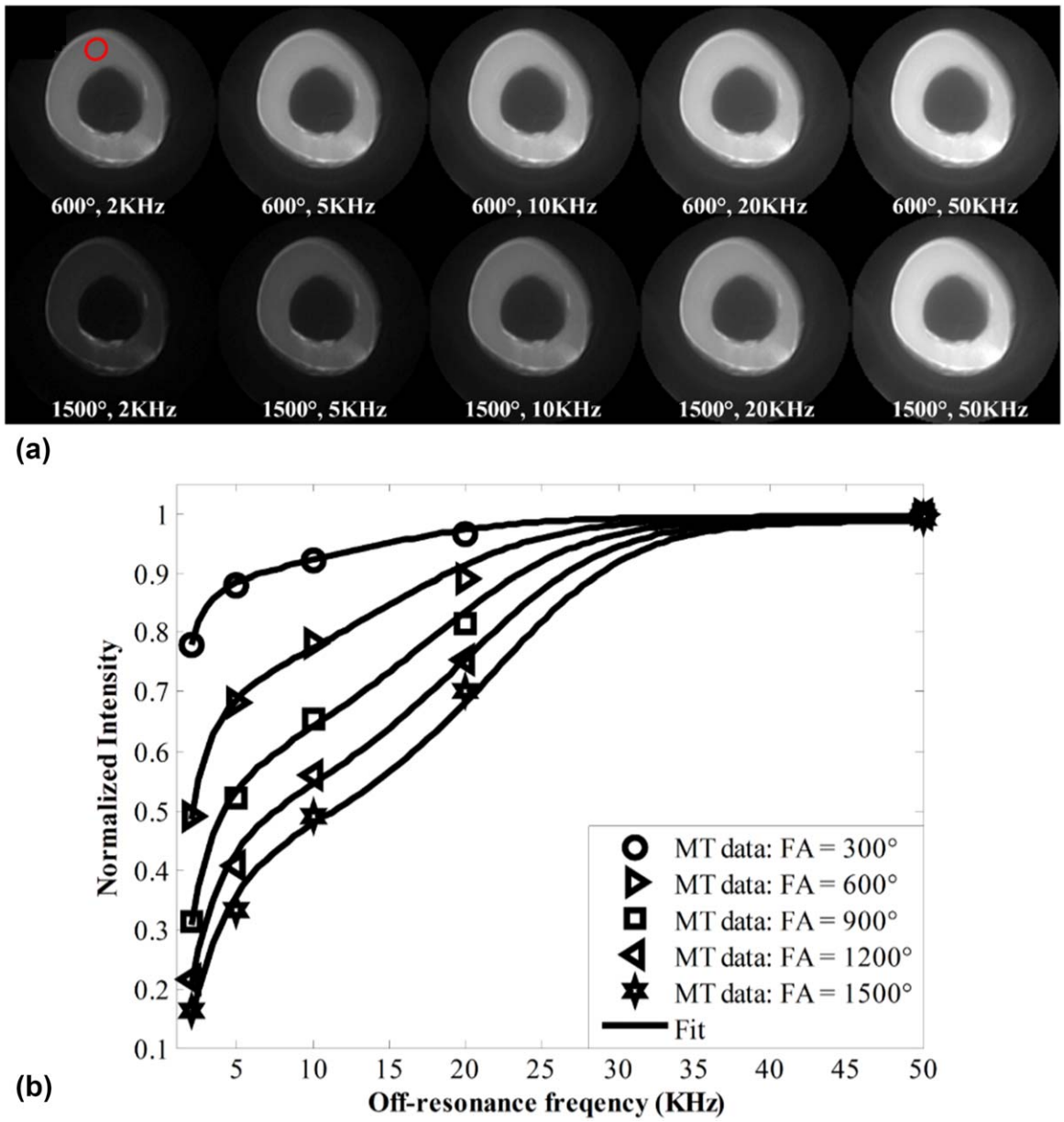

FIG. 1. (**a**) Representative MT images from an ex vivo bovine cortical bone specimen obtained with MT flip angles of 600° and 900° at increasing off-resonance frequencies of 2, 5,10, 20, and 50 kHz. (**b**) Fitting curves for cortical bone signal intensity versus off-resonance frequency for multiple MT flip angles are shown. Increased cortical bone signal intensity is observed at low MT flip angles and high off-resonance frequencies. Red circle in top left MT image (600°, 2 kHz) (**a**) shows region of interest used for signal intensity measurement.

two-pool modeling. Written informed consent approved by our Institutional Review Board was obtained before their participation in this study. An 8-channel knee coil was used for signal excitation and reception. The protocol was similar to that for the bovine specimens, except for the use of a soft half pulse excitation with variable rate selective excitation (pulse duration = 472 μs, pulse bandwidth = 2.7 kHz), field of view = $10 \times 10\,cm^2$, slice thickness of 7 mm, acquisition matrix = 192×192, and four MT powers (600°, 900°, 1200°, and 1500°) for a total scan time of 14 min. T_1 value was measured with a similar 2D selective UTE sequence (flip angle = 25°) and TRs = 10, 40, 70, 100, and 150 ms for a scan time of 2.6 min.

Data Analysis

The analysis algorithm was written in MATLAB 2012a (MathWorks, Natick, MA) and was executed offline on the DICOM images obtained by the 2D UTE-MT protocols described above. Two-pool UTE-MT modeling was carried out on the bovine femoral midshaft and human tibial midshaft cortical bones and was carried out pixel-wise (i.e., quantitative mapping) as well as by using the mean values of regions of interest placed in each image separately. Mean and standard deviation of macromolecular proton fractions, relaxation times, exchange rates, and water longitudinal relaxation rates were calculated and summarized.

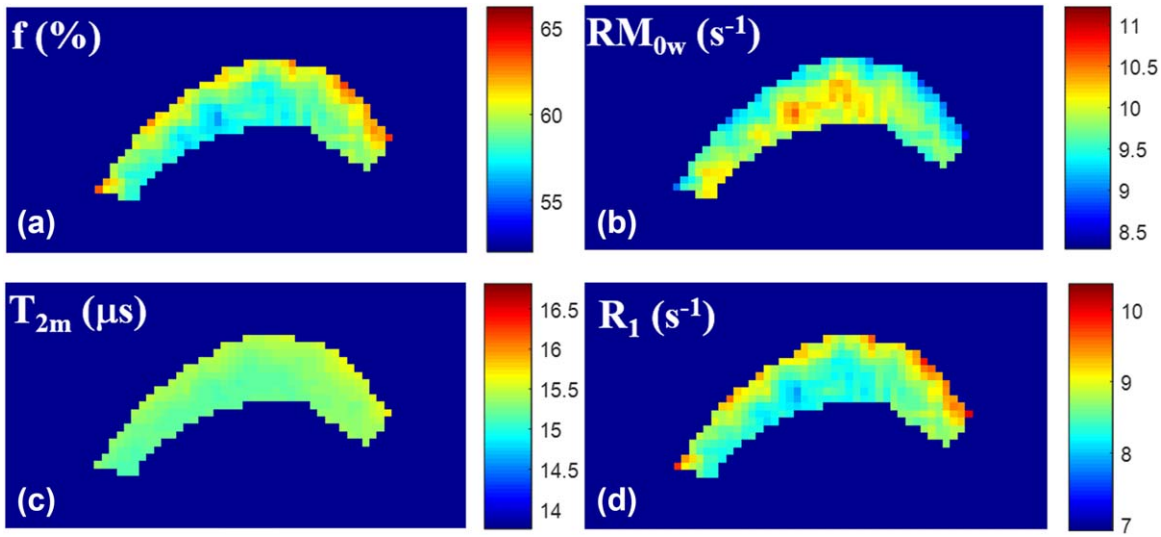

FIG. 2. Color mapping of MT modeling parameters from an ex vivo bovine cortical bone specimen, including macromolecular fraction (f) (**a**), proton exchange rate from the macromolecular to water pools (RM_{0w}) (**b**), T_2 relaxation time of the macromolecular pool (T_{2m}) (**c**), and spin-lattice relaxation rate of the water pool (R_{1w}) (**d**). Color maps demonstrate good homogeneity of MT modeling values within cortical bone. Color bar indicates the gradation of MT modeling measures.

RESULTS

Figure 1 shows 2D UTE-MT images from an ex vivo bovine cortical bone sample with different MT flip angles and off-resonance frequencies. Increased cortical bone signal intensity is observed at low MT flip angles and high off-resonance frequencies. The excellent fitting curves demonstrate the validity of using the 2D UTE-MT sequence to model MT effect in cortical bone that has extremely short T_2 and shows as signal void when imaged with conventional clinical sequences. Color maps of select MT modeling parameters from another bovine cortical bone specimen are presented in Figure 2. The parameter distributions of MT modeling can be seen in the analyzed region.

For the reproducibility study, mean and standard deviation values of three independent measurements for f, T_{2m}, R_{1w}, RM_{0m}, and RM_{0w} were $56.1 \pm 1.0\%$, 14.2 ± 0.02 s^{-1}, 16.9 ± 0.8 s^{-1}, 13.2 ± 0.1 s^{-1}, and 8.9 ± 0.4 s^{-1}, respectively, demonstrating excellent reproducibility of the 2D UTE-MT modeling technique.

UTE-MT images from in vivo human cortical bone are shown in Figure 3. Representative images at MT flips angles of 600° and 1500° show increased cortical bone signal intensity with lower MT power and higher off-resonance frequencies. Again, excellent curve fitting was achieved for all 2D UTE-MT data acquired with different MT flip angles and off-resonance frequencies, suggesting the feasibility for fast MT modeling of cortical bone in vivo.

Quantitative MT modeling measurements of ex vivo and in vivo cortical bone are presented in Tables 1 and 2, respectively. Mean bovine cortical bone values for f, T_{2m}, R_{1w}, RM_{0m}, RM_{0w}, and residual of fitting were $59.9 \pm 7.3\%$, 14.6 ± 0.3 μs, 9.9 ± 2.4 s^{-1}, 17.9 ± 3.6 s^{-1}, 11.8 ± 2.0 s^{-1}, and $1.8 \pm 0.1\%$, respectively. Mean human cortical bone values for f, T_{2m}, R_{1w}, RM_{0m}, RM_{0w}, and residual of fitting were $54.5 \pm 4.9\%$, 15.4 ± 0.6 μs, 8.9 ± 1.1 s^{-1}, 11.5 ± 3.5 s^{-1}, 9.5 ± 1.9 s^{-1}, and $2.7 \pm 0.3\%$, respectively.

Figure 4 shows the results of the sequential air-drying study. f, RM_{0m} and R_{1w} were increased with longer drying time. In addition, almost no changes were observed in T_{2m}.

DISCUSSION

In this study, we demonstrated that a quantitative model of MT can be carried out in ex vivo bovine and in vivo human cortical bone with suitable estimates of model parameters. We found the two-pool model to appropriately describe the acquired signal as a function of off-resonance RF power and frequency with good fit.

Several pools of proton signal in cortical bone have been identified, which differ considerably in their transverse relaxation times. Horch et al. (20) postulated six biophysical origins of nuclear magnetic resonance signals in cortical bone, including collagen methylene, collagen amides/hydroxides, mineral hydroxides/water, collagen-bound water, pore space water, and lipid methylene. Because most MRI techniques of cortical bone are dominated by signal from collagen-bound water and to a lesser extent pore water, most prior studies have focused on these proton pools (21–23). Several studies have shown that cortical porosity, such as from increased bone turnover or age-related bone loss, is a major determinant of bone mechanical strength (24–28). Hence, identifying potential surrogate measures of cortical porosity has been an area of considerable interest, especially using UTE techniques. For example, subsequent in vivo studies have validated the use of UTE MRI techniques for the assessment of bound and pore water (29,30). More recently, UTE MRI has been combined with UTE-MT to not only assess cortical bone water, but also the extremely short T_2 macromolecular proton pool (15,31).

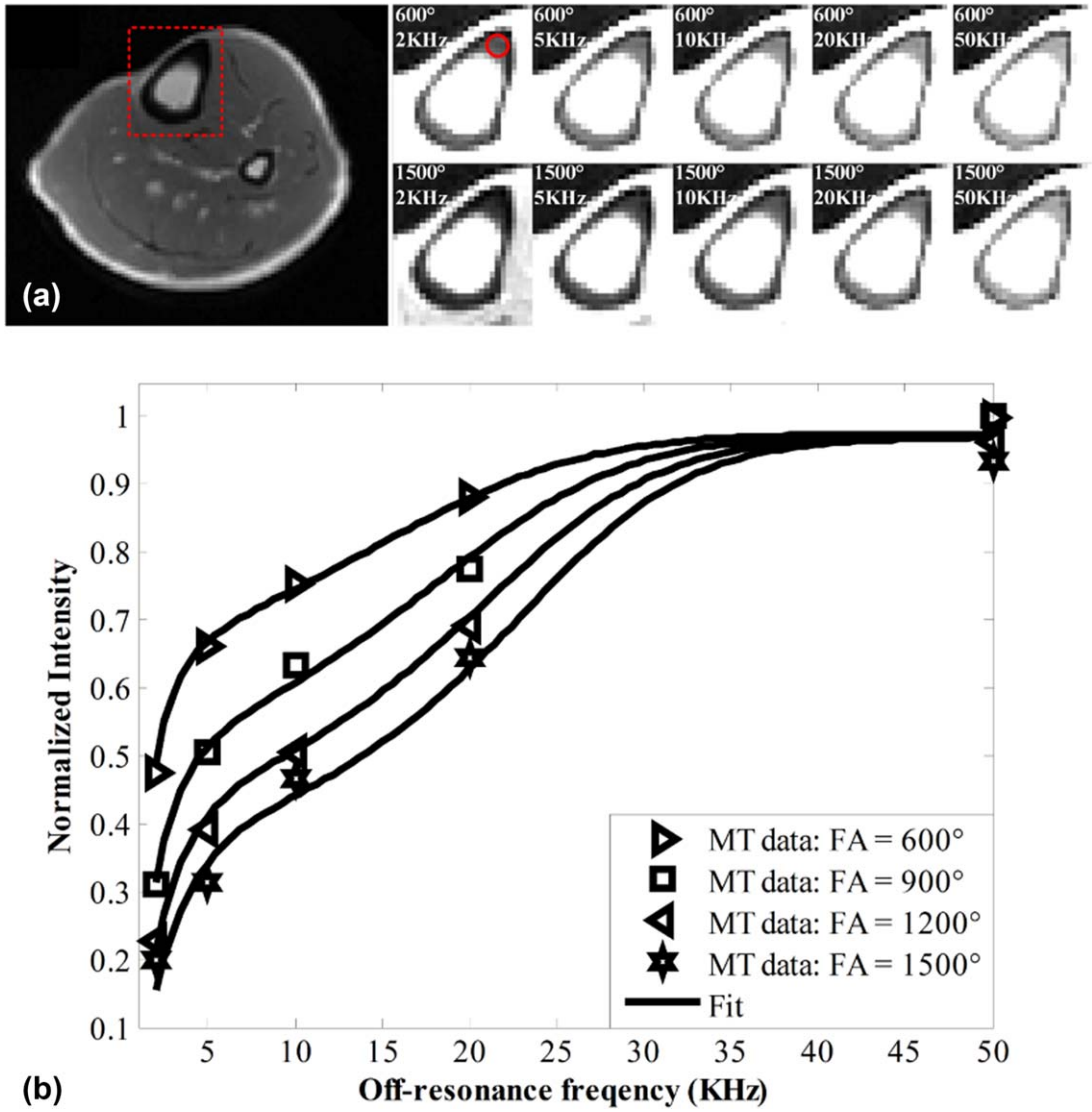

FIG. 3. (**a**) Representative MT images from in vivo human tibial cortical bone obtained with MT flip angles of 600° and 900° at increasing off-resonance frequencies of 2, 5, 10, 20, and 50 kHz. (**b**) Fitting curves for cortical bone signal intensity versus off-resonance frequency for multiple MT flip angles are shown. Similar to bovine cortical bone, increased signal intensity is evident at low MT flip angles and high off-resonance frequencies. Red dashed box in far-left image (**a**) shows field of view selection for MT analysis. Red circle in top left MT image (600°, 2 kHz) (**a**) shows region of interest used for signal intensity measurement.

Table 1
Quantitative MT Modeling Measurements for Ex Vivo Bovine Cortical Bone ($n = 5$).

	f (%)	T_{2m} (μs)	R_{1w} (s^{-1})	RM_{0m} (s^{-1})	RM_{0w} (s^{-1})	Residuals (%)
1	57.4	14.5	8.9	15.5	11.5	1.7
2	59.6	14.7	9.5	16.2	11	1.7
3	71.4	14.8	13.9	24.3	9.7	1.9
4	59.6	14.7	9.4	17.2	11.7	1.8
5	51.5	14.1	7.6	16.1	15.2	1.9

Abbreviations: f, macromolecular fraction; T_{2m}, T_2 relaxation time of macromolecular pool; R_{1w}, spin-lattice relaxation rate of water pool; RM_{0m}, proton exchange rate from water to macromolecular pool; RM_{0w}, proton exchange rate from macromolecular to water pool; Residuals, residual of fitting. The first column represents the sample index number.

Table 2
Quantitative MT Modeling Measurements for In Vivo Human Tibial Cortical Bone ($n = 5$).

	f (%)	T_{2m} (μs)	R_{1w} (s^{-1})	RM_{0m} (s^{-1})	RM_{0w} (s^{-1})	Residuals (%)
1	61.3	15.5	10.6	13.6	8.6	2.9
2	54.2	16.0	9.4	8.6	7.3	2.3
3	51.1	15.6	8.1	10.1	9.7	2.8
4	48.8	15.5	7.8	8.8	9.3	2.5
5	56.9	14.4	8.7	16.6	12.5	2.9

Abbreviations: f, macromolecular fraction; T_{2m}, T_2 relaxation time of macromolecular pool; R_{1w}, spin-lattice relaxation rate of water pool; RM_{0m}, proton exchange rate from water to macromolecular pool; RM_{0w}, proton exchange rate from macromolecular to water pool; Residuals, residual of fitting. The first column represents the volunteer index number.

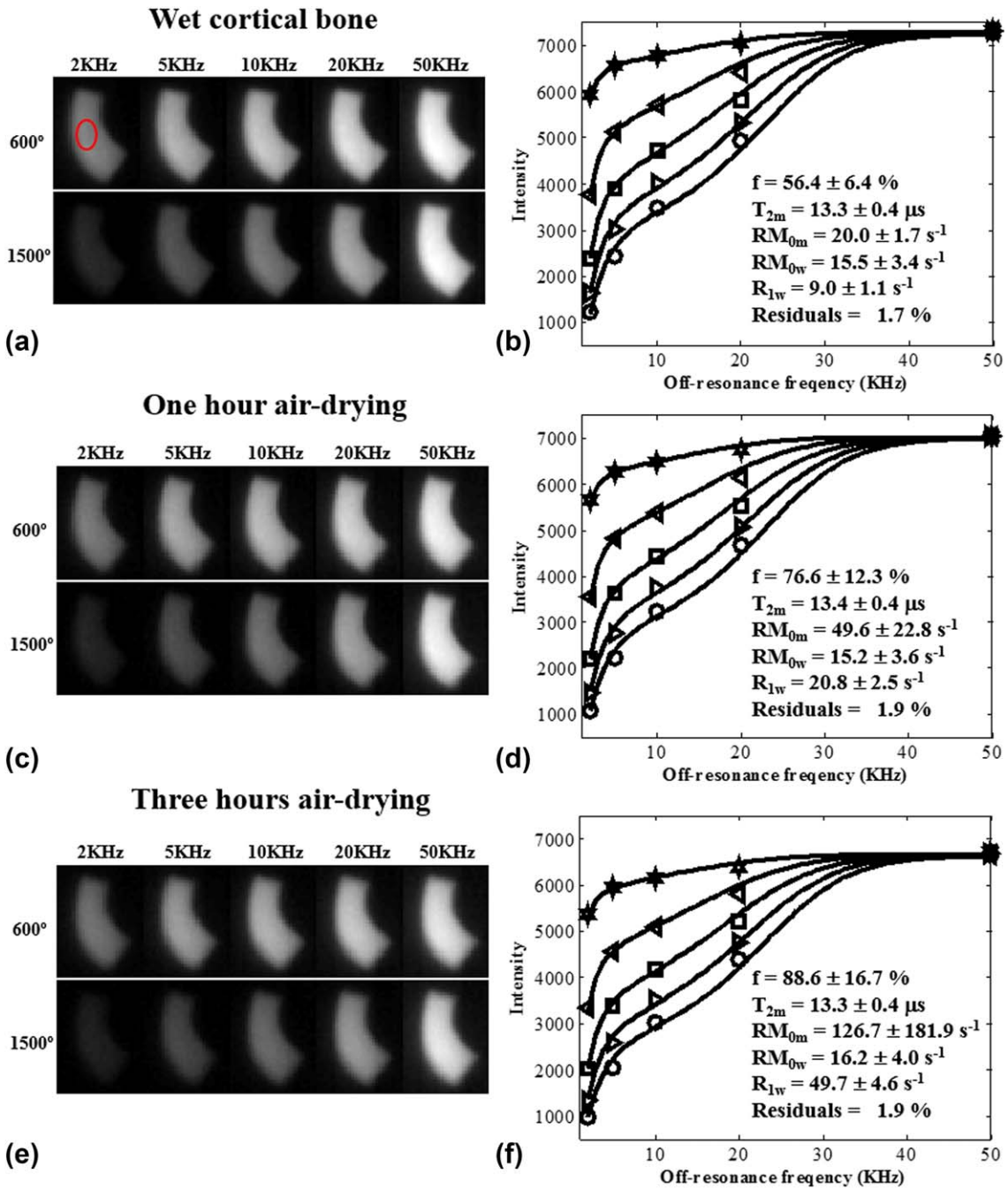

FIG. 4. (**a**), (**c**), and (**e**) are representative MT images from the sequential air-drying bovine cortical bone study (i.e., wet bone, 1 h of drying, and 3 h of drying) obtained with MT flip angles of 600° and 900° at increasing off-resonance frequencies of 2, 5,10, 20, and 50 kHz. (**b**), (**d**), and (**f**) are corresponding fitting curves for cortical bone signal intensity versus off-resonance frequency for multiple MT flip angles are shown. Red circle in top left MT image (600°, 2 kHz) (**a**) shows region of interest used for signal intensity measurement. The sequential MT modeling results are also shown in (**b**), (**d**), and (**f**).

Despite the potential advantages of UTE-MT over other methods of bone quantification, UTE-MT measurements are intrinsically semi-quantitative (14). Several variables can influence MTR, including main magnetic field and RF homogeneities, inherent tissue T_1 and T_2 relaxation times, and pulse sequence application. Well established in central nervous system applications (32,33), models detailing the MT process have been developed that are implementation-independent with few recent studies describing this technique in musculoskeletal applications, such as in Achilles tendon and muscle (17,34). To our knowledge, however, UTE-MT using two-pool modeling has not been previously reported in cortical bone.

Quantitative UTE-MT parameters obtained were f, T_{2m}, R_{1w}, RM_{0m}, and RM_{0w}. Previous studies show that all the MT modeling parameters are independent and can be uniquely determined (15,16). These parameters are

expected to provide information on various tissue properties. Higher MT powers can saturate macromolecular protons more effectively, allowing more accurate MT modeling. However, proper consideration should be given to the MT powers that are used because higher MT power will generate higher specific absorption ratio, which can be problematic, especially for in vivo studies. Powers up to 1500° with a TR of 100 ms represents a good balance between high saturation efficiency and specific absorption ratio limitation for in vivo imaging of the tibial midshaft. For MT modeling, the acquired data with a wide range of saturation including high saturation to non-saturation conditions are needed for accurate modeling because there are a total of five fitting parameters. The macromolecular components have a broad line shape with a T_2 around a few microseconds. Therefore, a wide range of off-resonance frequencies from 2 KHz to 50 KHz and MT powers from 300° to 1500° can generate a broad range of signal saturation. To achieve relatively accurate MT modeling, the lowest off-resonance frequency is chosen to minimize direct saturation of the water pool. Therefore, the lowest off-resonance frequency for MT modeling of short T_2 tissues such as cortical bone (minimal off-resonance frequency offset of 2 KHz) is higher than that of long T_2 tissues such as white matter and optic nerve (i.e., 1 KHz).

The bound or macromolecular fraction is a measure particularly unique to quantitative MT modeling. We observed mean macromolecular fractions of $59.9 \pm 7.3\%$ and $54.5 \pm 4.9\%$ in ex vivo bovine and in vivo human tibial cortical bone, respectively. The corollary of these results is in keeping with previous measures of total water content (17.4–24.8%) among in vivo human tibial cortical bone studies (10,35,36). Based on nuclear magnetic resonance signal experiments in human cortical bone, >80% of signal contributions from this observed proton fraction would be expected to correspond with collagen methylene (20). Because serum and urine collagen degradation products seen with increased bone resorption may be confounded by various factors such as circadian rhythm, fracture healing, and others (37), cortical bone bound fraction might be complementary to existing methods used for treatment monitoring and fracture risk prediction. The disease-specificity of such a measure, however, must be determined in patient studies before forming a conclusion on the clinical use of quantitative UTE-MT in cortical bone.

For the sequential air-drying study, f, RM_{0m}, and R_{1w} are increased with longer drying time. f is increasing as a result of more water loss with a longer drying time. With air-drying, free water can be lost much more quickly than bound water (38). As a result, bound water will represent a higher fraction of the water pool. Besides, exchange rates R, RM_{0m}, and R_{1w} of bound water content are higher than those of free water content. Both RM_{0m} and R_{1w} increase with longer drying time. No significant change in RM_{0w} was observed because of the compromise of the increasing R and decreasing M_{0w}. There is no change in T_{2m} because the short period of air drying does not affect the macromolecular proton pool much. Further air-drying studies would be interesting to investigate the changes of free water, bound water, and macromolecular proton contents when combined with UTE-MT modeling and UTE bi-component analysis (38).

The five MT modeling parameters including f, T_{2m}, R_{1w}, RM_{0m}, and RM_{0w} can be potentially useful biomarkers, especially considering that those biomarkers are insensitive to the magic angle effect (17). Conventional T_2 and T_{1rho} may increase by several fold when the collagen fibers are reoriented from 0° to 55° (the magic angle) relative to the B_0 field (39), while the MT modeling parameters are relatively constant with <10% increase near the magic angle (17). The UTE-MT modeling parameters may be useful in the diagnosis and treatment monitoring of osteoporosis, in which the macromolecular proton fraction is expected to inversely correlate with cortical porosity. Other MT modeling parameters such as relaxation times and exchange rates may also be correlated with bone properties. Further validation studies on cortical bone samples to correlate UTE MT modeling parameters with micro-CT measurements (cortical porosity, bone mineral content, and bone mineral density) and biomechanics including elastic (modulus, yield stress, and strain) and failure (ultimate stress, failure strain, and energy) properties are still under investigation. The fitted parameter T_{2w} is known to be less accurate, as has been discussed in greater detail in (40). Lack of consideration of the excitation pulse for this MT model and low duty cycle of the UTE-MT sequence as a result of specific absorption ratio limitation can both lead to inaccurate T_{2w} estimation. For 2D UTE-MT modeling of cortical bone, T_{2w} may be subject to increased error because of the simplification of both bound water and free water into a single water pool. T_{2w} can be easily measured by a fast multi-echo UTE sequence. The curves did not fit the experimental data perfectly, which is probably because of the two-pool approximation. In fact, there are many proton pools in bone tissues including a free water pool, a bound water pool, and a macromolecular pool. Therefore, a two-pool model may not be accurate but just a reasonable approximation in which bound water and free water are simplified as one water pool. In addition, there were also biases between the fitting curves and the experimental data for 2D UTE-MT modeling. However, these biases were also present in the Ramani model, which was used to evaluate the cerebral cortex and a multiple sclerosis (MS) lesion (see Fig. 2 in 15). Although a slight fitting bias exists, their results show that the MT modeling parameters can be good biomarkers to distinguish between normal white matter and MS lesions. We hope the 2D UTE-MT modeling parameters can similarly provide clinically useful biomarkers of cortical bone properties such as cortical porosity and biomechanical properties. Clearly, a lot more research remains to be carried out.

Fat has a much higher signal intensity than cortical bone and will also lead to off-resonance and Gibbs ringing artifacts. Therefore, the MT modeling parameters may be affected by fat. Recently, Smith et al. (41) reported that with increased fat fraction, both macromolecular fractions and exchange rates are decreased but T_2 relaxations are increased by numerical simulation. To reduce the fat contamination induced errors, they

incorporate Dixon multi-echo fat-water separation for fat-free MT modeling. Incorporating fat-water separation methods into UTE-MT modeling can potentially resolve this issue and will be investigated in future studies.

Simulations have been carried out to investigate the effects of B_1 inhomogeneity on MT modeling. From our simulations, if B_1 changes by 5%, the T_1 value measured with the variable TR method will change by 9.3% and MT parameters including f, RM_{0m}, RM_{0w}, and R_{1w} will change by 2.3%, 8.9%, 12.9%, and 8.7%, respectively. There is almost no change for T_{2m}. Therefore, B_1 variation can lead to increased errors in MT quantification, especially for RM_{0m}, RM_{0w}, and R_{1w}. On the other hand, a smaller degree of error is observed for f and T_{2m} as a result of B_1 inhomogeneity. To fully address the errors induced by B_1 variation, correction techniques are needed for accurate MT quantification with a measured B_1 map (42).

There are several limitations to this study. First, we had a small sample size for both ex vivo and in vivo groups. Second, imaging time was clinically prohibitive and longer compared to other bone water quantification methods, including semi-quantitative UTE-MT MTR measurements (12,14,37). Some potential strategies to reduce scan time for clinical use include using fewer data sets, selecting MT powers and frequency offsets using Cramer-Rao lower bounds theory (43), and compressed sensing reconstruction (44). Third, consideration must be given to the level of RF power deposition generated by acquiring MT data at different MT pulse powers and off-resonance frequencies. This may ultimately impact the dynamic range of quantitative UTE-MT acquisitions. Last, most of the previously reported quantitative MT models assume only two pools of protons (water and macromolecular protons) (13,15,16), theoretically, however, a three-pool model (free water, bound water, and macromolecular protons) would be more accurate than the two-pool model for evaluating biological tissues (45).

In conclusion, we provided preliminary data for UTE-MT modeling in ex vivo bovine and healthy adult cortical bone. This technique allows for a more comprehensive assessment of the MT process than previously reported by MTR measurement alone and lays the ground work for future studies into disease-based changes in MT parameters. We believe that UTE-MT modeling has the potential to provide a complementary quantitative approach to the diagnosis and treatment of conditions associated with impaired bone quality.

REFERENCES

1. Nazrun AS, Tzar MN, Mokhtar SA, Mohamed IN. A systematic review of the outcomes of osteoporotic fracture patients after hospital discharge: morbidity, subsequent fractures, and mortality. Ther Clin Risk Manag 2014;10:937–948.
2. Johnell O, Kanis J. Epidemiology of osteoporotic fractures. Osteoporosis Int 2005;2(Suppl 16):S3–S7.
3. Cummings SR, Karpf DB, Harris F, Genant HK, Ensrud K, LaCroix AZ, Black, DM. Improvement in spine bone density and reduction in risk of vertebral fractures during treatment with antiresorptive drugs. Am J Med 2002;112:281–289.
4. Schuit SC, van der Klift M, Weel AE, de Laet CE, Burger H, Seeman E, Hofman A, Uitterlinden AG, van Leeuwen JP, Pols HA. Fracture incidence and association with bone mineral density in elderly men and women: the Rotterdam Study. Bone 2004;34:195–202.
5. Sornay-Rendu E, Munoz F, Garnero P, Duboeuf F, Delmas PD. Identification of osteopenic women at high risk of fracture: the OFELY study. J Bone Miner Res 2005;20:1813–1819.
6. Majumdar S, Genant HK, Grampp S, Newitt DC, Truong VH, Lin JC, Mathur A. Correlation of trabecular bone structure with age, bone mineral density, and osteoporotic status: in vivo studies in the distal radius using high resolution magnetic resonance imaging. J Bone Miner Res 1997;12:111–118.
7. Reichert IL, Robson MD, Gatehouse PD, He T, Chappell KE, Holmes J, Girgis S, Bydder GM. Magnetic resonance imaging of cortical bone with ultrashort TE pulse sequences. Magn Reson Imaging 2005;23:611–618.
8. Bae WC, Chen PC, Chung CB, Masuda K, D'Lima D, Du J. Quantitative ultrashort echo time (UTE) MRI of human cortical bone: correlation with porosity and biomechanical properties. J Bone Miner Res 2012;27:848–857.
9. Du J, Carl M, Bydder M, Takahashi A, Chung CB, Bydder GM. Qualitative and quantitative ultrashort echo time (UTE) imaging of cortical bone. J Magn Reson 2010;207:304–311.
10. Techawiboonwong A, Song HK, Leonard MB, Wehrli FW. Cortical bone water: in vivo quantification with ultrashort echo-time MR imaging. Radiology 2008;248:824–833.
11. Henkelman RM, Stanisz GJ, Graham SJ. Magnetization transfer in MRI: a review. NMR Biomed 2001;14:57–64.
12. Syha R, Martirosian P, Ketelsen D, Grosse U, Claussen CD, Schick F, Springer F. Magnetization transfer in human Achilles tendon assessed by a 3D ultrashort echo time sequence: quantitative examinations in healthy volunteers at 3T. RoFo 2011;183:1043–1050.
13. Hodgson RJ, Evans R, Wright P, Grainger AJ, O'Connor PJ, Helliwell P, McGonagle D, Emery P, Robson MD. Quantitative magnetization transfer ultrashort echo time imaging of the Achilles tendon. Magn Reson Med 2011;65:1372–1376.
14. Chang EY, Bae WC, Shao H, et al. Ultrashort echo time magnetization transfer (UTE-MT) imaging of cortical bone. NMR Biomed 2015;28:873–880.
15. Ramani A, Dalton C, Miller DH, Tofts PS, Barker GJ. Precise estimate of fundamental in-vivo MT parameters in human brain in clinically feasible times. Magn Reson Imaging 2002;20:721–731.
16. Henkelman RM, Huang X, Xiang QS, Stanisz GJ, Swanson SD, Bronskill MJ. Quantitative interpretation of magnetization transfer. Magn Reson Med 1993;29:759–766.
17. Ma YJ, Shao H, Du J, Chang EY. Ultrashort echo time magnetization transfer (UTE-MT) imaging and modeling: magic angle independent biomarkers of tissue properties. NMR Biomed 2016;29:1546–1552.
18. Du J, Bydder GM. Qualitative and quantitative ultrashort-TE MRI of cortical bone. 2013;26:489–508.
19. Chen J, Chang EY, Carl M, Ma Y, Shao H, Chen B, Wu Z, Du J. Measurement of bound and pore water T1 relaxation times in cortical bone using three-dimensional ultrashort echo time cones sequences. Magn Reson Med 2017;77:2136–2145.
20. Horch RA, Nyman JS, Gochberg DF, Dortch RD, Does MD. Characterization of 1H NMR signal in human cortical bone for magnetic resonance imaging. Magn Reson Med 2010;64:680–687.
21. Biswas R, Bae W, Diaz E, Masuda K, Chung CB, Bydder GM, Du J. Ultrashort echo time (UTE) imaging with bi-component analysis: bound and free water evaluation of bovine cortical bone subject to sequential drying. Bone 2012;50:749–755.
22. Nyman JS, Ni Q, Nicolella DP, Wang X. Measurements of mobile and bound water by nuclear magnetic resonance correlate with mechanical properties of bone. Bone 2008;42:193–199.
23. Ong HH, Wright AC, Wehrli FW. Deuterium nuclear magnetic resonance unambiguously quantifies pore and collagen-bound water in cortical bone. J Bone Miner Res 2012;27:2573–2581.
24. McCalden RW, McGeough JA, Barker MB, Court-Brown CM. Age-related changes in the tensile properties of cortical bone. The relative importance of changes in porosity, mineralization, and microstructure. J Bone Joint Surg Am 1993;75:1193–1205.
25. Ahmed LA, Shigdel R, Joakimsen RM, Eldevik OP, Eriksen EF, Ghasem-Zadeh A, Bala Y, Zebaze R, Seeman E, Bjørnerem Å. Measurement of cortical porosity of the proximal femur improves identification of women with nonvertebral fragility fractures. Osteoporosis Int 2015;26:2137–2146.

26. Schaffler MB, Burr DB. Stiffness of compact bone: effects of porosity and density. J Biomech 1988;21:13–16.
27. Nyman JS, Roy A, Tyler JH, Acuna RL, Gayle HJ, Wang X. Age-related factors affecting the postyield energy dissipation of human cortical bone. J Orthop Res 2007;25:646–655.
28. Basillais A, Bensamoun S, Chappard C, Brunet-Imbault B, Lemineur G, Ilharreborde B, Ho Ba Tho MC, Benhamou CL. Three-dimensional characterization of cortical bone microstructure by microcomputed tomography: validation with ultrasonic and microscopic measurements. J Orthop Sci 2007;12:141–148.
29. Rajapakse CS, Bashoor-Zadeh M, Li C, Sun W, Wright AC, Wehrli FW. Volumetric cortical bone porosity assessment with MR imaging: validation and clinical feasibility. Radiology 2015;276:526–535.
30. Manhard MK, Horch RA, Gochberg DF, Nyman JS, Does MD. In vivo quantitative MR imaging of bound and pore water in cortical bone. Radiology 2015;277:927.
31. Springer F, Martirosian P, Machann J, Schwenzer NF, Claussen CD, Schick F. Magnetization transfer contrast imaging in bovine and human cortical bone applying an ultrashort echo time sequence at 3 Tesla. Magn Reson Med 2009;61:1040–1048.
32. Ridha BH, Tozer DJ, Symms MR, Stockton KC, Lewis EB, Siddique MM, MacManus DG, Rossor MN, Fox NC, Tofts PS. Quantitative magnetization transfer imaging in Alzheimer disease. Radiology 2007; 244:832–837.
33. Tozer D, Ramani A, Barker GJ, Davies GR, Miller DH, Tofts PS. Quantitative magnetization transfer mapping of bound protons in multiple sclerosis. Magn Reson Med 2003;50:83–91.
34. Sinclair CD, Samson RS, Thomas DL, Weiskopf N, Lutti A, Thornton JS, Golay X. Quantitative magnetization transfer in in vivo healthy human skeletal muscle at 3 T. Magn Reson Med 2010;64:1739–1748.
35. Li C, Seifert AC, Rad HS, Bhagat Y, Rajapakse CS, Sun W, Lam SC, Wehrli FW. Cortical bone water concentration: dependence of MR imaging measures on age and pore volume fraction. Radiology 2014; 272:796–806.
36. Rad HS, Lam SC, Magland JF, Ong H, Li C, Song HK, Love J, Wehrli FW. Quantifying cortical bone water in vivo by three-dimensional ultra-short echo-time MRI. NMR Biomed 2011;24:855–864.
37. Unnanuntana A, Gladnick BP, Donnelly E, Lane JM. The assessment of fracture risk. J Bone Joint Surg Am 2010;92:743–753.
38. Biswas R, Bae W, Diaz E, Masuda K, Chung CB, Bydder GM, Du J. Ultrashort echo time (UTE) imaging with bi-component analysis: bound and free water evaluation of bovine cortical bone subject to sequential drying. Bone 2012;50:749–755.
39. Shao H, Pauli C, Li S, Ma Y, Tadros AS, Chang EY, Du J. Magic angle effect plays a significant role in T1rho relaxation in articular cartilage. Osteoarthritis Cartilage 2017. doi: 10.1016/j.joca.2017.01.013.
40. Cercignani M, Barker GJ. A comparison between equations describing in vivo MT: the effects of noise and sequence parameters J Magn Reson 2008;191:171–183.
41. Smith AK, Dortch RD, Dethrage LM, Lyttle BD, Kang H, Welch EB, Smith SA. Incorporating novel quantitative magnetization transfer of the human optic nerve in vivo. Magn Reson Med 2017;77:707–716.
42. Yarnykh VL. Optimal radiofrequency and gradient spoiling for improved accuracy of T1 and B1 measurements using fast steadystate techniques. Magn Reson Med 2010;63:1610–1626.
43. Cercignani M, Alexander DC. Optimal acquisition schemes for in vivo quantitative magnetization transfer MRI. Magn Reson Med 2006; 56:803–810.
44. Lustig M, Donoho D, Pauly JM. Sparse MRI: the application of compressed sensing for rapid MR imaging. Magn Reson Med 2007;58: 1182–1195.
45. Ceckler T, Maneval J, Melkowits B. Modeling magnetization transfer using a three-pool model and physically meaningful constraints on the fitting parameters. J Magn Reson 2001;151:9–27.